New Light on Old Manuscripts, VB 45, 419–429

https://doi.org/10.1553/978OEAW91575s419

Leif Glaser

X-Ray Fluorescence Investigations on Iron Gall Ink Writing: Equipment and Geometry

INTRODUCTION

Iron gall ink, as the dominant writing material in Europe and the Middle East for the last two millennia, is of key interest when dealing with historic documents. If documents need to be placed within a historical frame of reference, context, hands, and languages used can be sufficient, but materials analysis may add conclusive information or confirm earlier assessments. In some cases, only modern methods of investigation allow for a definitive answer to a question. Among the methods predominantly used, X-ray fluorescence (XRF) spectroscopy is a versatile tool for analyzing metallic components in an object's surface and thin inhomogeneous films.[1] In the case of written documents, for XRF investigations the objects (a page at a time) can be assumed to consist entirely of a surface area. Due to an increasing variety of equipment in use and results presented, a better basis to work from in order to compare independent measurements is increasingly important.

This paper will present some factors that influence XRF results on iron gall ink measurements and will demonstrate how some of these can be utilized to explore specific questions. The equipment discussed will be limited to energy dispersive XRF, which is useful for elemental characterization of a sample. It will be noted that wavelength dispersive XRF systems can additionally identify the chemical environment of the metal, but require much longer times for the respective measurement, while chemical and compound information can also be obtained faster by Raman measurements. While some discrepancies in the XRF results are intrinsic to the differences in the systems used, some are simply of geometrical origin and affect each system. This paper will start by introducing the different general types of equipment available today and listing their key characteristics, while highlighting their intrinsic differences and impact on measurements. This section is then followed by a discussion of general geometric issues when dealing with thin film samples (such as inks) and which settings need to be documented. Not every object allows an identical approach. Even when using the same system on two similar objects, changes in geometry may influence the results. Finally, some remarks are made concerning standards and metadata. Since most historic documents are in less than perfect condition, transporting them to large-scale facilities for investigation is usually undesirable, so experiments are performed at the site where the object is kept. Due to the resulting importance of transportable equipment in dealing with cultural heritage, the focus of the paper is therefore on transportable equipment of this type. Moreover, specific treatment or sampling to optimize measurement is typically out of the question when measuring unique historic objects, and thus samples with untreated surfaces are presupposed here. All Monte Carlo calculations were done using the XMI-MSIM code,[2] which uses the Ebel model for the X-ray tube spectra.[3]

METHODS AND EQUIPMENT

To perform XRF measurements on iron gall ink writing, many different kinds of equipment can be used. There is a huge variety of handheld XRF (hXRF) systems that are all shaped handgun-like and can be used in point and shoot mode, mounted on tripods, or attached to desktop chambers. These hXRF scanners have been primarily developed for quality control in metal production, geological probing,[4] and screening for toxic ele-

Leif Glaser: Universitätsklinikum Hamburg-Eppendorf, Onkologisches Zentrum, Klinik für Strahlentherapie und Radioonkologie, Labor für Strahlenbiologie, Martinistr. 52, D-20246 Hamburg; le.glaser@uke.de

[1] Markowicz *et al.*, Method; Sitko, Quantitative X-ray fluorescence analysis.

[2] Schoonjans *et al.*, Monte-Carlo Simulation.

[3] Ebel, Tube spectra.

[4] Norrish and Hutton, An accurate x-ray spectrographic method; Potts and Webb, X-ray fluorescence spectrometry; Rowe *et al.*, The

ments. The systems are optimized for their main purpose—e.g. trace element detection in a metallic matrix, soil, or rock sample. In the last decade, several companies have adjusted their tools for use in cultural heritage investigations, but the workhorse application driving the developments remains unchanged. Primary uses of these hXRF spectrometers are in general field tests and pilot surveys. The second group of XRF equipment comprises laboratory systems that are mainly benchtop machines and have a much more diverse primary use than the handheld spectrometers. There are several systems on the market that have been optimized or even specifically built for cultural heritage investigations, after the usefulness of the technique had been demonstrated in a srXRF test case.[5] These spectrometers are primarily used for, and for most samples and questions they give high quality results, while they are still transportable enough to be relocated to objects that cannot be transported themselves. The last group of XRF 'systems' are large-scale facilities. They either deliver ion beams (for particle induced X-ray emission: PIXE[6]) or X-ray beams (synchrotron radiation XRF: srXRF). These methods allow high-resolution, high-quality analysis of material with the lowest detection limit for a non-invasive technique,[7] but they cannot be moved to an object. There are many similarities between the first two groups of systems compared with the third, as shown in Table 1. The differences between hXRF (1) and lab-XRF (2) appear rather subtle, but in some cases are significant when comparing results.

	(1) Handheld	**(2) Benchtop**	**(3) Large-scale facility**
Spot size	1–8 mm	30 µm–1 mm	10 nm–1 mm
Flux	10^6–10^7 ph/s	10^7–10^9 ph/s	10^{10}–10^{14} ph/s
Detector area	6–50 mm²	50–120 mm²	variable
Photon source	X-ray tube	X-ray tube	Undulator
Photons	Poly-chromatic	Poly-chromatic	Monochromatic
Filters	optional	standard	Not needed
Sample environment	Air	Air/Helium/Vacuum	Air/Helium/Vacuum
Weight	1.5–3.0 kg	50–500 kg	>> 30 000 t
Mobility	Mobile	Transportable	Stationary
Retail price	20–80 k€	80–300 k€	200–500 M€
Price per 10^6 ph/s	8000–20 000 €	3000–8000 €	1–2 €

Tab. 1: Three different groups of XRF systems: Handheld, benchtop, and large-scale facilities. The parameters listed give some idea of the size, price, and performance of the systems.

The most significant difference between today's X-ray lab equipment and large-scale facilities is the source of the X-rays. While any lab equipment uses some sort of an X-ray tube with variable anode material, large-scale facilities use magnetic fields and electron beams to produce X-rays. The spectra produced by Undulator and X-ray tube are very different. Undulator radiation is monochromatic and can be tuned to a desired energy in the operation range of the undulator (e.g. 6 keV to 60 keV).[8] Undulator radiation[9] is usually linear polarized and thus allows specific geometries, where the background for XRF measurements is especially low. X-ray tube radiation (Fig. 1+2), on the other hand, has a broad energy spectrum and consists of two main contributions: a continuous acceleration voltage-depending Bremsstrahlungs-spectrum, and an anode material-depending characteristic line spectrum. The radiation is unpolarized and intrinsically poly-chromatic, while filters can easily be applied with moderate flux reduction (Fig. 1+2) to reduce unwanted radiation; a post source polari-

quantification.

5 Dik *et al.*, Visualization; Bergmann, Imaging.

6 For the scope of this paper, PIXE is concidered a monochromatically excited storage ring based XRF method primarily for light metals.

7 'Non-invasive technique' is defined in this context as a method that requires neither sampling (not even micro sampling) nor any physical contact with the object, while also not measurably changing or damaging the object due to the investigation.

8 Due to the tunability and monochromaticity of the photon energy of undulator radiation, there is no need for filter foils, except sometimes for a different function as absorbers for flux reduction.

9 Margaritondo, Synchrotron Light.

zation reduces the flux one to two orders of magnitude. The spectrum of a typical X-ray tube has a significant (30%–50%) contribution in the energy range below the iron K edge, which reduces the effective flux that is useful for iron gall ink investigations by almost this amount. Additionally, the lower energy part of the X-ray spectrum is more strongly absorbed by the parchment and thus slightly more harmful to the document investigated.[10] The most common solution to this is the use of a filter to absorb the low energy part of the spectrum. In the case of iron gall ink measurements, aluminum (Fig. 1+2) is the best suited filter material, as aluminum is cheap to produce in any thin foil thickness and most effective in suppressing only the low energy side of the spectrum (X-ray attenuation length taken from NIST database[11]).

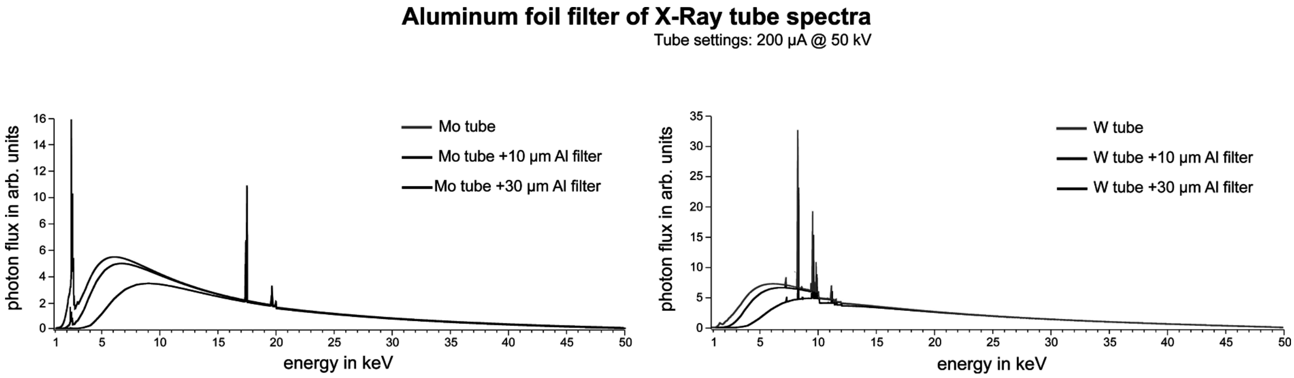

Fig. 1: The spectra of an X-ray tube with an anode material of molybdenum (left) and tungsten (right) and the effect of a 10 µm and 30 µm aluminum filter on the two spectra.

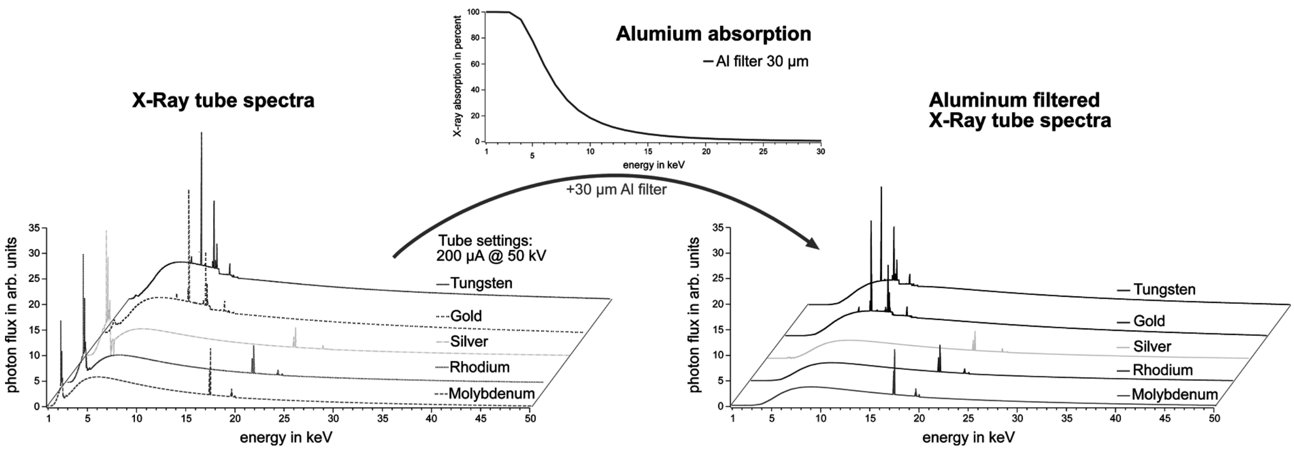

Fig. 2: A spectral overview of the 5 most common X-ray tube anode materials is shown on the left. The tubes setting is in the order of a typical setting for a handheld XRF device. The energy dependence of the absorption for aluminum is shown top center. On the right side the spectra from the left have been filtered with a 30 µm aluminum filter.

The X-ray tubes can be operated at different acceleration voltages and different anode currents. These settings change the shape of the produced spectrum: while the anode current predominantly changes the intensity (flux) of the tube, the acceleration voltage influences the shape of the spectrum. As shown in Figure 3 (left) an

[10] Young, *Effect.*
[11] henke; NIST.

X-ray tube with tungsten anode material is varied only at the anode current while keeping the acceleration voltage fixed at 50 kV: the intensity of the spectrum increases while the relative percentage of the entire spectrum that is e.g. below the iron absorption edge (7.112 keV) stays constant at 23%. Likewise, the spectral center of gravity[12] stays constant at 12.2 keV. Changing the anode current is therefore a safe option that can be adjusted if necessary, while performing a set of measurements. Any change of the anode current will thus influence only the time duration for the measurements, but not any relative intensities within the measured XRF data. The opposite is true when the acceleration voltage is changed, as shown in Figure 3 (middle and right), while the anode current is fixed at 500µA: the shape of the spectrum changes with the acceleration voltage, consequently the relative amount of the respective spectra above the iron absorption edge ranges from 57% at 20 kV acceleration voltage to 87% at 80 kV. In the same way the spectral center of gravity shifts from 7.9 keV at 20 kV to 18.1 keV at 80 kV. This holds true to a different extent for every absorption edge in the energy range of the X-ray tube's spectrum. Any change of the acceleration voltage within a series of measurements will affect the relative amount of the elements detected. If this tube is to be used to measure an historic document to e.g. identify an iron gall ink metallic fingerprint,[13] an acceleration voltage of at least 50 kV is advisable in order to have sufficient flux at the iron, copper, zinc and lead edges.

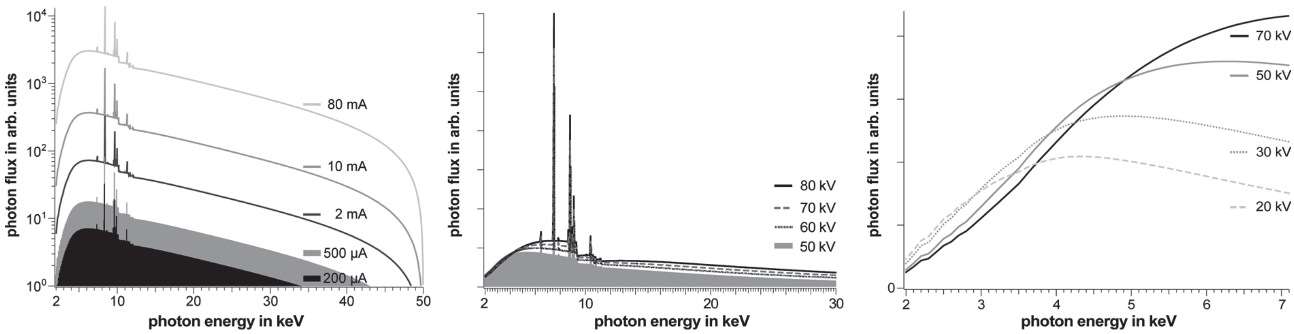

Fig. 3: The effect of varying the anode current on a tungsten X-ray tube with fixed acceleration voltage of 50 kV (left) is simply the increase of flux. When keeping the anode current fixed, but varying the acceleration voltage (middle and right), the shape and thus spectral center of gravity changes. The higher the acceleration voltage, the harder the mean X-rays emitted from the tube.

Obviously changing between two tubes with different anode materials can have significant effects on the resulting data too. For the same iron gall ink, the characteristic metallic fingerprint of the ink may appear differently. Take molybdenum and tungsten as popular anode materials (Fig. 1): while the characteristic lines of molybdenum are above all absorption edges that usually appear in an iron gall ink, tungsten's most intensive characteristic line (W Lα @ 8.4 keV) is below the copper (9.0 keV), zinc (9.7 keV), and lead absorption edges (up to 15.2 keV). Hence an ink fingerprint determined with a molybdenum and a tungsten anode tube system will differ: if the measurement with the tungsten tube would lead to relative amounts in respect to iron of e.g. 9% Ca, 71% Cu and 5% Zn, the same ink could show 10% Ca, 73% Cu and 5% Zn with a molybdenum tube of otherwise identical settings (50 kV / 0.2mA / no filter), if no compensation is done. The mathematical relation between two different fingerprints measured of the same sample of element X in respect to iron is:

$$\frac{X_2}{Fe_2} = \left(\frac{X_1}{Fe_1}\right) \cdot \left(\frac{I_{(X_2)}}{I_{(X_1)}}\right) \cdot \left(\frac{I_{(Fe_1)}}{I_{(Fe_2)}}\right)$$

12 I.e. energy value where half of the delivered photons in the spectrum are above and half of them are below the energy.
13 Malzer *et al.*, A fingerprint; Hahn *et al.*, Iron-gall inks.

Where X_2/Fe_2 is the element X to iron ratio of the second measurement, X_1/Fe_1 that from the first measurement, while $I(Fe_1)$, $I(Fe_2)$, $I(X_1)$ and $I(X_2)$ are the spectral flux contributions above the absorption edge of the elements Iron and X of tubes 1 and 2. The effects of changes in the spectra due to anode material, acceleration voltage, and filters can be cumulative. While for ink fingerprint analysis, comparable results can be expected if molybdenum, rhodium, or silver tubes are used, while gold and tungsten may over- or under-represent a trace element relative to measurements with the other three anode materials. Companies use calibration curves for their systems to compensate for these effects, but they usually do not share them with the customer. What is more, most cultural heritage samples do not strictly meet an industrial standard, hence a margin for error remains. A systematic comparison of different systems and different tube settings on clearly-defined reference samples is highly recommendable. In spite of any compensation effort, lines corresponding to the characteristic X-ray lines of the anode material remain present in the measured data. If the anode is made out of a standard material such as, e.g., molybdenum, rhodium, or tungsten, it is easy to correct for these measurement artefacts simply by ignoring them when dealing with cultural heritage objects. All three metals were discovered between 1778 and 1803 and should not show up in any measurement of historic objects. These metals are very uncommon impurities in historic material and were not deliberately used for cultural heritage objects after their discovery. Two other common anode materials for X-ray tubes are silver and gold and inherently not favorable for cultural heritage investigation systems. Both metals were widely used in art and illustrations for several thousand years and will show up regularly when measuring historic material, although neither metal is present in any iron gall ink.

Measurements from a large-scale facility are more easily used as reference, due to the monochromatic, polarized nature of the X-rays used.[14] There is only one energy present, and if that is given, the energy-dependent absorption cross-section for each detected element can be looked up (NIST). This way, results achieved at different excitation energies can be compared. For an exact comparison between measurements from tube-based systems and large-scale facilities the measurement of an identical standard with both approaches is best.[15]

MEASUREMENT AND SAMPLE GEOMETRY

A lot of the systems on the market are sold without exact information on their performance, as e.g. the actual photon flux is often considered a company secret, hence a comparison of advertised systems of different companies is difficult.[16] Nevertheless, there are several general effects on the sample investigation that will be discussed here first: the angle of incidence and angle of detection, as well as the spot size, all in relationship to the key feature of interest, may severely affect the results obtained. The simplest effect is the angle of incidence, which has less influence for solid materials, but changes the interaction length with thin films geometrically (Fig. 4):

$$I_l = d/sin\,(\alpha)$$

Where d is the thickness of the material, α the angle of incidence (90° as incidence normal to the surface), and I_l the interaction length in the material. Changing the angle of incidence, while keeping the detector at a fixed position, can be used to determine the thickness of a layer or the existence of a layered system in the first place. While a homogeneous object will appear the same at different illumination angles, the elements from a coating or surface layer will appear to be twice as abundant under 30° incidence than under 90°. A more grazing incidence will in the same way elongate the X-ray footprint on the investigated surface and thus increase the spot size in that direction. An increased spot size has a limiting effect on the maximal lateral resolution achievable. The spot size can alsohave a distinctive effect on the measurement itself, as the size relative to the region of interest is the main variable (Fig. 5).

[14] Glaser and Deckers, Basics.
[15] Chen *et al.*, High Definition.
[16] The flux listed in Table 1 for the different groups of XRF systems is not from the companies selling the systems, but from companies producing the X-ray tubes that are usually installed in those systems.

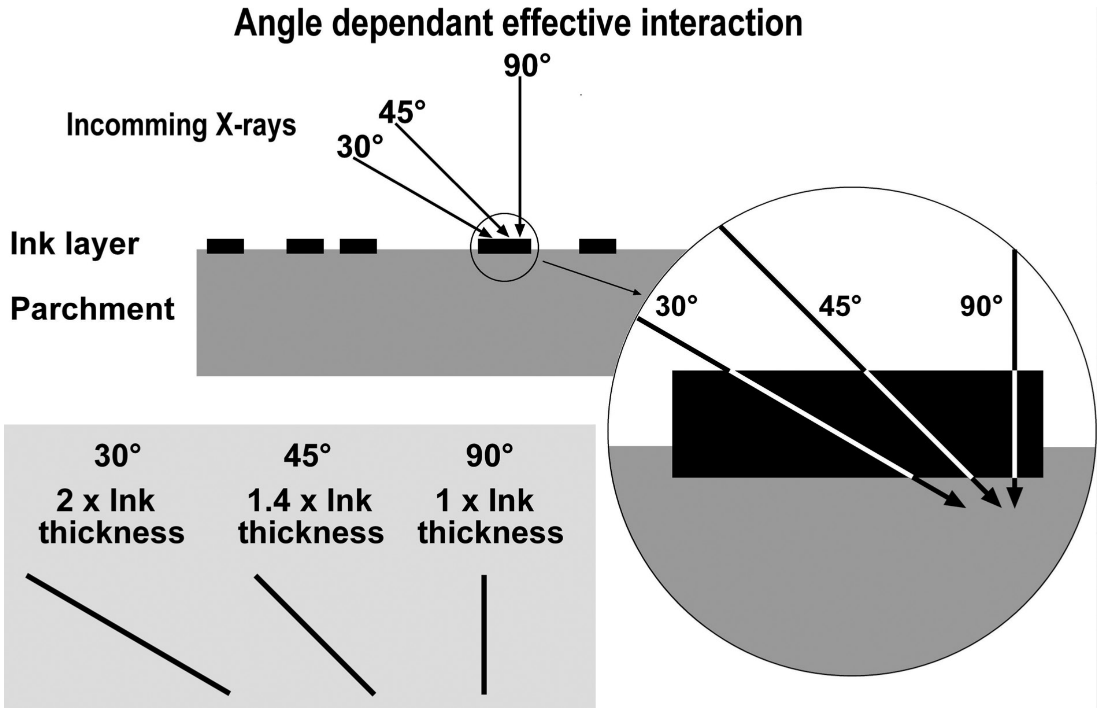

Fig. 4: The angle dependent interaction length is simply a geometric effect. The more grazing the incidence of the photons is, the longer the effective interaction length with the ink. By the same measure, the X-ray footprint on the object is increased and the potential lateral resolution decreases.

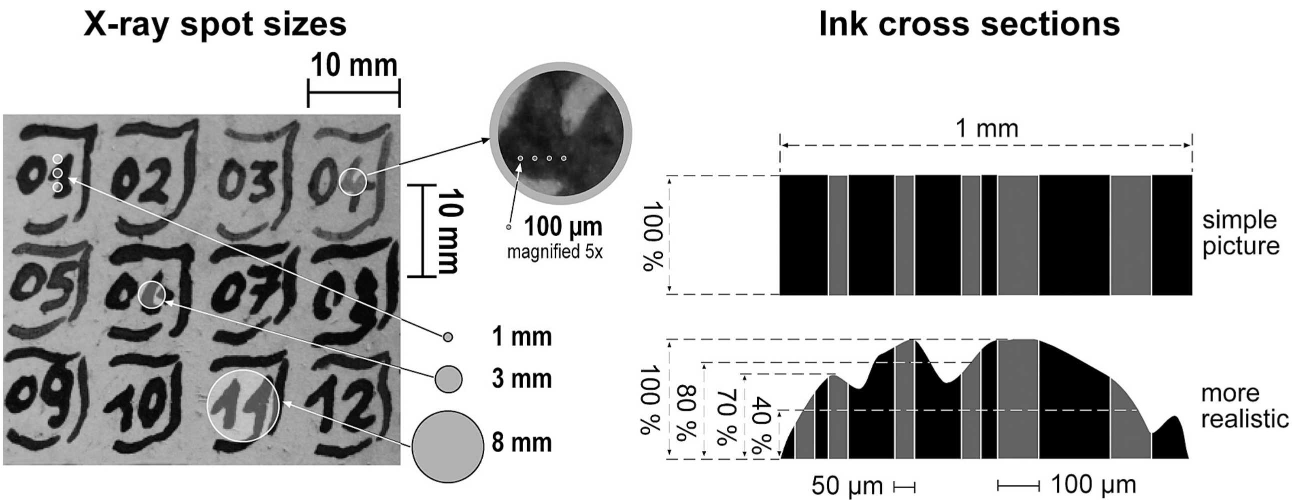

Fig. 5: Left: Reference object with 12 different iron gall inks and typical spot sizes used with hXRF systems (1–8 mm). — Top center: A 5x magnified section of the ink reference page to visualize the spotsize of typical benchtop XRF systems. These spot sizes are also commonly available at large-scale facilities. — Right: A uniform thick ink (top) and an ink of varying thickness (bottom) with the spot size dependent relative amount of ink measured.

An XRF signal from a homogeneous sample is constant in respect to spot size changes, as it was constant in respect to the angle of illumination. For the iron gall ink 11 (Fig. 5+6) on parchment the characteristic metallic fingerprint is to be examined.

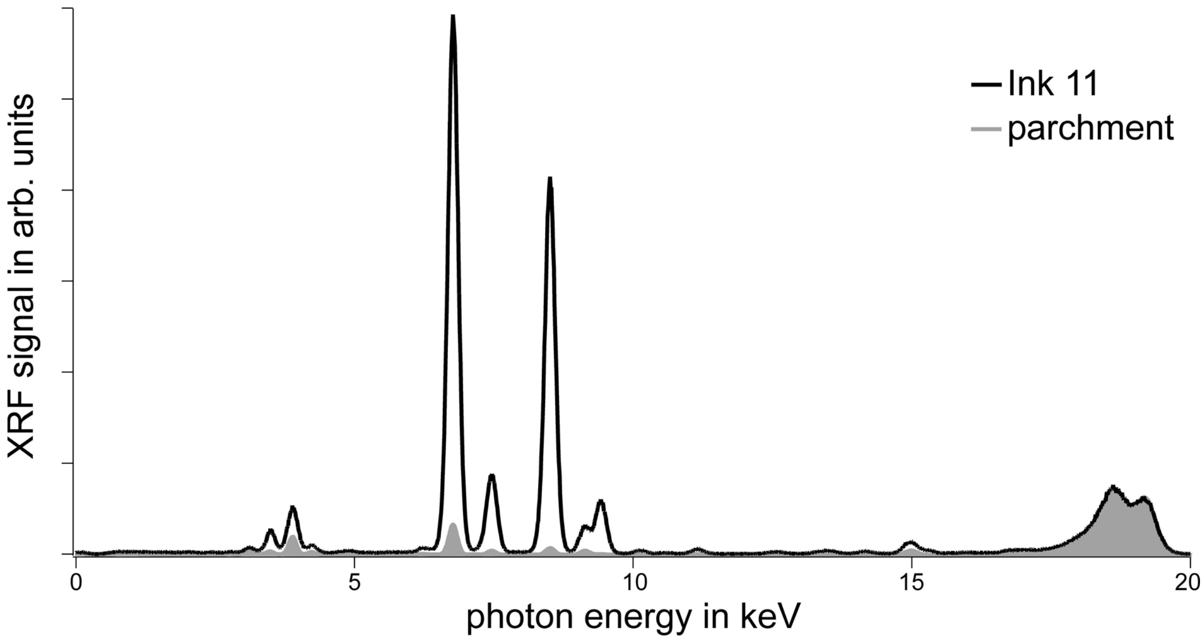

Fig. 6: The spectrum of the ink 11 and the parchment measured at a storage ring facility with 18 keV monochromatic X-rays.

If the spot size is large in respect to the region of interest, the measurement is a mean value of feature and background as e.g. the 8 mm spot will measure 60–80% just parchment (Tab. 2).

	Ca / Fe	**Cu / Fe**	**Zn / Fe**	**Pb / Fe**
Ink 11	0.09	0.71	0.05	0.01
Parchment	0.57	0.26	0.15	0.07
Ink 11 (80%) + parchment (20%)	0.10	0.70	0.05	0.01
Ink 11 (40%) + parchment (60%)	0.12	0.68	0.06	0.02
Ink 11 (20%) + parchment (80%)	0.17	0.63	0.07	0.02

Tab. 2: Metallic fingerprints derived from ink and parchment measurement and how that changes, when due to larger beams some areas are measured for the ink's metallic fingerprint where no ink is present.

With a smaller spot in the order of the region of interest, as e.g. the 3 mm spot being almost the size of the character, the measurement contains more ink, but still at least 20% parchment. The moment the spot size is in the order of the character line width (or smaller), the measurement is mainly or entirely of ink. This of course depends on the precision of the instrument to measure the region of interest as chosen.[17] The practical approach to avoid imprecision in alignment (even for better-adjustable devices) is to make small line scans across an ink's stroke. A second, usually unspoken, assumption is that the ink is very evenly spread within a stoke. This is of course a simplistic view, since the amount of ink on a quill is reduced in the writing process and thus the line thickness is continuously getting thinner until the quill is dipped into the ink again. The ink's cross-section is also not homogeneous at each given point, disappearing instantly at the edges (Fig. 5 top right), but has a variable cross-section. Ideally the ink thickness should be determined at each point of the measurement. This

[17] The hXRF instuments are rather hard to position exactly, while laboratory systems often have a microscope attached which helps to position the X-ray's field of view very precisely on a location on the sample.

is very unrealistic, since it would be too time consuming to remeasure each point inspected with XRF with a 3D microscope and attribute the right ink thickness to each measured point. A possible option for a potential intrinsic calibration of the measurement and to gain additional information on the ink thickness is to use the X-ray fluorescence lines' self absorption effects. Due to the slight energetic difference of the two emitted characteristic lines of iron, the lower energetic line (Fe Kα) is more strongly absorbed by the ink than the energetically higher line (Fe Kβ). The evaluation of the ratio of the two different lines makes it possible to determine thickness of the ink from which the X-rays were emitted. A Monte Carlo simulation with the XMI-MSIM code was performed: 17keV incoming monochromatic polarized X-rays hit an iron foil of varying thickness placed under 45°. The 300 µm thick silicon drift detector (SDD) was placed at 90° to the incoming beam in the plane of polarization and likewise at 45° to the thin film surface normal. The spectra analysis shows that there is an almost linear relationship for the iron peak ratio (Kα/Kβ) in thin iron foils of 0 to 10 µm.

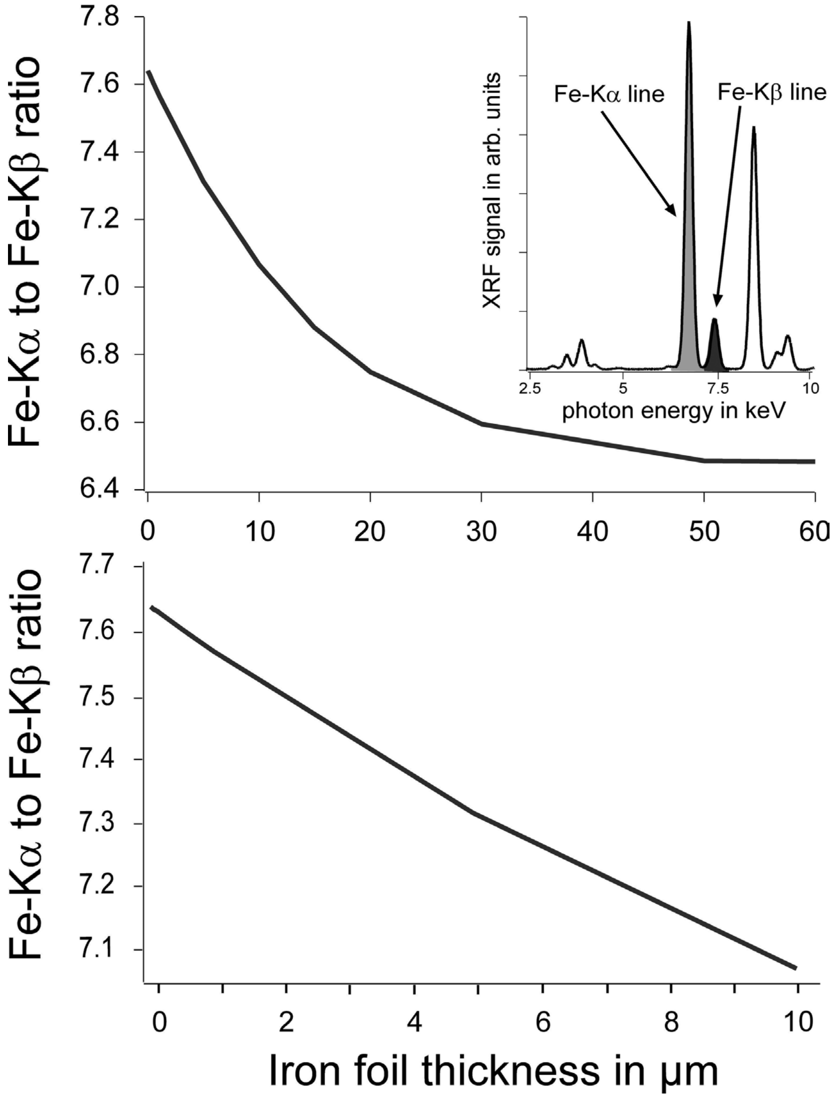

Fig. 7: The ratio of the two iron K-lines for thin iron films from 0 to 60 µm (top) and 0 to 10 µm (bottom). This ratio can be used as intrinsic thickness calibration.

Fe foil in µm	**Fe-Kα / Fe-Kβ**	**Estimated thickness of iron gall ink in µm**
0.001	7.64	0.014
0.01	7.64	0.14
0.05	7.64	0.7
0.1	7.63	1.4
0.5	7.60	7
1	7.57	14
5	7.31	70
10	7.07	140
15	6.88	210
20	6.75	280
30	6.60	420
50	6.49	700
100	6.47	1400
1000	6.47	14000

Tab. 3: Iron K-line peak ratio for thin iron films and the estimated thicknesses of iron gall ink that generates the same iron peak ratio in an XRF measurement.

With the black color of iron gall inks being a complex of Gallic acid and iron, the amount of iron is of course much less per thickness in ink than in an iron foil. Going through the numbers: 0,001 µm (1nm) is roughly three times the diameter of an iron atom. There are 28 atoms (hydrogen not counted) in an iron-tannin complex,[18] of which there are 2 iron atoms. As a first rough estimate, there is one iron layer for every 14 layers of the ink. At least 200 nm are needed for any system to be optically active, which corresponds to about 600–700 layers of bcc iron. Assuming significantly less density for ink than bcc iron, it might be some 200–300 layers of ink, and thus compare to 20 layers (1/14) of iron foil as calculated. This would correspond to 6 nm of thin film (Fe Kα to Fe Kβ ratio = 7.64). A reasonable iron gall ink thickness of 35 µm[19] corresponds to a 1 µm thin iron film (Fe Kβ to Fe Kα ratio = 7.57). The differences are subtle but distinct and due to noise in real systems the measuring time per point may become too long to use this approach as calibration method for each point. If the statistic for each point is insufficient, but enough points are measured on a document, a sum spectrum of all points measured can be generated and an average ink thickness determined. This mean value may help to cluster documents statistically. Changing the measuring geometry can be helpful if specific questions are addressed, as e.g. the thickness of a surface layer as discussed above. For the same reason, the measuring geometry should always be documented alongside the published results.

COMPARING DATA AND METADATA

Keeping a fixed setting (e.g. spot size, tube settings, etc.) in a laboratory environment is a safe option for operating in a closed environment to compare different samples measured there on a relative scale. Any comparison of results achieved under different operation conditions (e.g. other hardwaresettings, different type of system) will lead to uncertainties, as discussed above. As the number of investigated objects in the field of cultural heritage, including written documents, will increase significantly in the next decade, often more than one method will be applied to each investigated object, and not necessarily under exactly the same conditions. The more and specific information (metadata) about published investigations are available, the better it will be as a basis for future comparison and the cultural heritage community. In several fields, where extremely large amounts of data are produced, as in the storage ring facility community, workshops are held to discuss the best

[18] Krekel, *Chemische Untersuchungen.*
[19] Liu and Strlič, Kinetics.

way to handle and store metadata.[20] In the cultural heritage community, the need for this is significantly less pressing, but some guidelines should nevertheless be discussed here. It is important for any follow-up investigations that data already gathered relating to a specific object or reference material becomes and remains useful after the data has been published. Hence, alongside basic fundamental details, such as the type of system used, the entire settings list should be included: X-ray tube anode material, acceleration voltage, anode current, spot size, angle of incidence, angle of detection, distance to the object, support material, (if used) filter material and thickness, ideally even an X-ray spectrum of the source. Additionally, if used, helium flow or cryojets should always be mentioned. The software (including the version) used for evaluation should also be included. For better comparison of different results of different groups and spectrometers, measuring a standard reference material would be desirable. In the case of iron gall ink, a set of pure systems of the three main metallic 'ingredients' would be desirable, as $FeSO_4$, $CuSO_4$ and $ZnSO_4$ are not restricted chemicals and can be handled with no danger to the experimenter. Using 5g of each compound in 50ml of a saturated solution of Gallic acid in water will produce tinctures, which have reasonably similar amounts of metals to iron gall inks. A mixture of the three in e.g. equal parts applied to easily-available standardized paper such as whatman No1 would be a reference everyone can make and reproduce at any time, if needed. Only data published with sufficient information will benefit the cultural heritage community.

REFERENCES

Bergmann, Uwe, Chapter 6, Imaging with X-ray Fluorescence, in: Reviel Netz, William Noel, Natalie Tchernetska, and Nigel Wilson (eds.), *The Archimedes Palimpsest*, vol. 1 (Cambridge, 2011).

Chen, Zewu W., Walter M. Gibson, and Huapeng Huang, High Definition X-Ray Fluorescence: Principles and Techniques, *X-Ray Optics and Instrumentation* (2008) Article ID 318171, DOI: 10.1155/2008/318171 (accessed 01.07.2023).

Dik, Joris, Koen Janssens, Geert Van Der Snickt, Luuk van der Loeff, Karen Rickers, and Marine Cotte, Visualization of a Lost Painting by Vincent van Gogh Using Synchrotron Radiation Based X-ray Fluorescence Elemental Mapping, *Analytical chemistry* 80 (2008) 6436–6442.

Ebel, Horst, X-Ray Tube spectra, *X-Ray Spectrometry* 28/4 (1999) 255–266, DOI: 10.1002/(SICI)1097-4539(199907/08)28:4<255::AID-XRS347>3.0.CO;2-Y (accessed 01.07.2023).

Glaser, Leif and Daniel Deckers, Basics of fast scanning XRF element mapping for iron gall ink palimpsests, *Manuscript Cultures* 7 (2015) 104–112.

Grunzke, Richard, Jürgen Hesser, Jürgen Starek, Nick Kepper, Sandra Gesing, Marcus Hardt, Volker Hartmann, Stephan Kindermann, Jan Potthoff, Michael Hausmann, Ralph Müller-Pfefferkorn, and René Jäkel, Device-driven Metadata Management Solutions for Scientific Big Data Use Cases, in: *22nd Euromicro International Conference on Parallel, Distributed, and Network-Based Processing* (PDP 2014), DOI: 10.1109/PDP.2014.119 (accessed 01.07.2023).

Hahn, Oliver, Wolfgang Malzer, Birgit Kanngiesser, and Burkhard Beckhoff, Characterization of iron-gall inks in historical manuscripts and music compositions using X-ray fluorescence spectrometry, *X-Ray Spectrometry* 33 (2004) 234–239.

henke: http://henke.lbl.gov/optical_constants/atten2.html (accessed 01.07.2023).

Krekel, Christoph, *Chemische Untersuchungen an Eisengallustinten und Anwendung der Ergebnisse bei der Begutachtung mittelalterlicher Handschriften*, Master's Thesis, Institut für Anorganische Chemie der Georg-August-Universität zu Göttingen (1990).

Liu, Yun, Irena Kralj Cigić, and Matija Strlič, Kinetics of accelerated degradation of historic iron gall ink-containing paper, *Polymer Degradation and Stability* 142 (2017) 255–262, DOI: 10.1016/j.polymdegradstab.2017.07.010 (accessed 01.07.2023).

lsdma: https://www.aifb.kit.edu/web/LSDMA (accessed 01.07.2023).

Malzer, Wolfgang, Oliver Hahn, and Birgit Kanngiesser, A fingerprint model for inhomogeneous ink-paper layer systems measured with micro-X-ray fluorescence analysis, *X-Ray Spectrometry* 33 (2004) 229–233, DOI: 10.1002/xrs.676 (accessed 01.07.2023).

[20] Grunzke *et al.*, Metadata Management; lsdma.

Markowicz, Andrzej, Nikolaus Hasselberger, and U. Whai Zin Oo, Method for Quantitative XRF Analysis of Inhomogeneous Thin Specimen, *X-Ray Spectrometry* 22 (1993) 160–162.

Margaritondo, Giorgio, Synchrotron Light in a Nutshell, *Surface Review and Letters* 7/4 (2000) 379–387, DOI: 10.1142/S0218625X00000488 (accessed 01.07.2023).

NIST: https://physics.nist.gov/PhysRefData/FFast/html/form.html (accessed 01.07.2023).

Norrish, Keith and John T. Hutton, An accurate x-ray spectrographic method for the analysis of a wide range of geological samples, *Geochimica et Cosmochimica Acta* 33 (1969) 431–453.

Potts, Philip J. and Peter C. Webb, X-ray fluorescence spectrometry, *Journal of Geochemical Exploration* 44 (1992) 251–296.

Rowe, Harry, Niki Hughes, and Krystin Robinson, The quantification and application of handheld energy-dispersive x-ray fluorescence (ED-XRF) in mudrock chemostratigraphy and geochemistry, *Chemical Geology* 324–325 (2012) 122–131, DOI: 10.1016/j.chemgeo.2011.12.023 (accessed 01.07.2023).

Schoonjans, Tom, Lazslo Vincze, Vicente Armando Solé, Manuel Sanchez del Rio, Karen Appel, and Claudio Ferrero, A General Monte-Carlo Simulation of Energy-Dispersive X-ray-Fluorescence Spectrometers Part 6. Quantification through iterative simulations, *Spectrochimica Acta Part B* 82 (2013) 36–41, DOI: 10.1016/j.sab.2012.12.011 (accessed 01.07.2023).

Sitko, Rafał, Quantitative X-ray fluorescence analysis of samples with less than ‘infinite thickness’: Difficulties and possibilities, *Spectrochimica Acta Part B: Atomic Spectroscopy* 64/11–12 (2009) 1161–1172, DOI: 10.1016/j.sab.2009.09.005 (accessed 01.07.2023).

Young, Gregory, *Effect of High Flux X-radiation on Parchment, Report No. Proteus 92195* (Canadian Conservation Institute, 2005).

http://www.archimedespalimpsest.org/pdf/archimedes_f.pdf (accessed 01.07.2023).